RC connections strengthened with FRP sheets using grooves on the surface

A.R. Sattarifard[1], M.K. Sharbatdar[2,*], A. Dalvand[3]

Abstract

In this paper, an experimental study has been conducted on strengthening of reinforced concrete (RC) connections by FRP sheets. The innovation of this research is using narrow grooves on critical regions of connection to increase the adherence of FRP sheets and prevent their early debonding. Therefore, four RC connections were made and tested under a constant axial load on the column and an increasing cyclic load on the beam. The first specimen, as the standard reference specimen, had close tie spacing in ductile regions of beam, column and panel zone based on seismic design provisions, and the second specimen, as the weak reference specimen did not have these conditions in all regions. Two other weak specimens were strengthened using two different strengthening patterns with FRP sheets; one by ordinary surface preparation and the other with surface grooving method for installing FRP sheets on the connection. The results showed that ultimate load and ductility of the weak specimen compared to standard specimen decreased 25% and 17%, respectively. The shear failure and concrete crushing were prevented in the ductile regions of the beam and panel zone in both strengthened specimens. Also, it was observed that early debonding of FRP sheets was prevented in the strengthened connection with grooving pattern and so had desirable ductility and bearing capacity similar to the standard specimen.

Keywords: RC connection, Strengthening, FRP sheets, Load capacity, Surface grooving, Debonding.

1. Introduction

For supplying adequate ductility of reinforced concrete (RC) members and connections, special requirements are considered in design codes. Close tie spacing in the panel zone and critical regions of beam and column for increasing their ductility are among these important requirements [1-2]. These seismic and ductility requirements have not been considered in some of RC structures designed and built based on the old design codes in the recent fifty years, so shear failure was observed in many members like panel zones due to reduction of concrete confinement and ductility. Therefore, structure strengthening is necessary to prevent probable damages during earthquakes [3-5]. One of the most common solutions for rehabilitation of RC frames is confining column and panel zone to a new concrete with the longitudinal and transversal reinforcements [6].

Another technique for repairing damaged RC frames is evacuating the concrete core of beam-column connection, and then filling it with high strength no-shrinkage mortar

(70 MPa) or using HPFRCC[1] for strengthening RC frames or epoxy pressure injection technique [7-11].

Rehabilitation techniques of external epoxy-bonded steel plates or steel prop and curb method were widely used to increase the ductility of joints [12-14]. FRP sheets were used to improve many concrete elements such as columns particularly for seismic rehabilitation [15]. More recently, FRP sheets and CFRP rods (in NSM[2] method) have been used in bending and shear rehabilitation of RC connections [16-17] in order to increase load bearing capacity, ductility and other parameters of connections [18-28]. Usually, these sheets are installed locally on one or some faces of RC members with ordinary surface preparation method [29-30], but still there is high probability of early debonding of FRP sheets from concrete surface before rupturing at ultimate tensile strength (strain) [31-33]. Grooving the concrete surface before installing sheets is one of the newest surface preparation methods to increase the adherence between sheets and concrete surface [34].

In this study, the effects of ties spacing (in panel zone and critical regions of the beam and column) on behavior and failure of connections are studied. Also, two retrofitting patterns with FRP sheets are used for strengthening weak connections. Their beneficial effects (compared to weak and standard connections) are investigated. Furthermore, ordinary surface preparation and grooving method are used for installation of sheets, so

* Corresponding author: msharbatdar@semnan.ac.ir

1 Graduated MS of Structural Engineering, Semnan University, Semnan, Iran
2 Associate Professor, Faculty of Civil Engineering, Semnan University, Semnan, Iran
3 Assistant professor, Faculty of Engineering, Lorestan University, Khorramabad, Iran

as an important result of paper, beneficial effects of grooves for postponing the early debonding of sheets are investigated.

2. Experimental Program

Four external RC beam-column connections were designed, fabricated and tested under cyclic loading, up to their ultimate load bearing capacity and ductility, stiffness degradation and energy absorption were evaluated. The first two connections were considered as reference specimens and other connections were strengthened with FRP sheets. For installing FRP sheets, ordinary surface preparation and surface grooving methods were performed in 1st and 2nd strengthened connections, respectively.

2.1. Material properties

In all specimens, cement type II (ASTM type II) and angular aggregate up to 10 mm were used for making C30 concrete[3]. So 357 kg of cement, 160.7 kg of water, 678.6 kg of dry sand and 1143 kg of dry stone were mixed for making 1m^3 concrete. Accordingly concrete cylinder strength of 7 and 28-days-old were 23 and 31 MPa, respectively. In columns, yielding and ultimate strength of longitudinal reinforcements[4] were 510 and 588 MPa and those in beams were 444 and 677 MPa, respectively. Also these parameters for tie reinforcements were 398 and 586 MPa, respectively. Mechanical properties of CFRP sheets used for strengthening of connections were Tensile strength, Elastic modulus, Ultimate tensile strain and thickness per layer equal to 3550 MPa, 235 GPa, 1% and 0.11 mm, respectively.

2.2. Specimens details

General details of specimens are given in Fig. 1. The moderate ductility requirements of design codes for ties in critical regions of beam, column and panel zone were performed at the standard reference specimen (SR), while these requirements were not considered in other three weak connections (unstrengthened weak reference specimen, WR, and two strengthened specimens of RW1 and RW2, using two different patterns with FRP sheets). For installing FRP sheets in specimens RW1 and RW2, ordinary and grooving surface preparation methods were performed, respectively. In specimen RW1, member's surface was cleaned completely, then a layer of epoxy resin was put on the concrete surface and filled all pores in order to obtain a completely smooth surface. But grooving method was used in specimen RW2 for installing FRP sheets by cutting some grooves with specific dimension on the surface and then filling them by an early layer of epoxy resin to get a complete smooth and uniform surface. These grooves increase contact surface between epoxy resin and concrete, so bonding strength of FRP sheets with concrete surface is increased [34]. Grooves were cut parallel to the fibers direction in order to increase bonding strength between sheets and concrete and to have a better stress distribution between grooves, epoxy resin and fibers. Dimension, direction and location of grooves on the connection are shown in Fig. 2. Grooves are vertically at both sides of beam (perpendicular to the beam axis) and horizontally at both sides of panel zone (parallel to the beam axis). These grooves were cut over 400 mm of critical region of the beam. According to Fig. 3, grooves have 4 mm width and 8 mm depth with center to center of 30 mm.
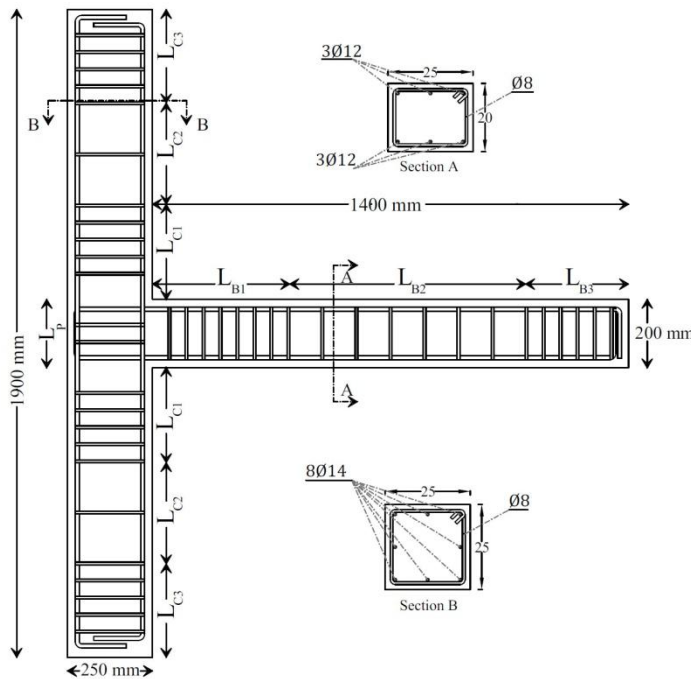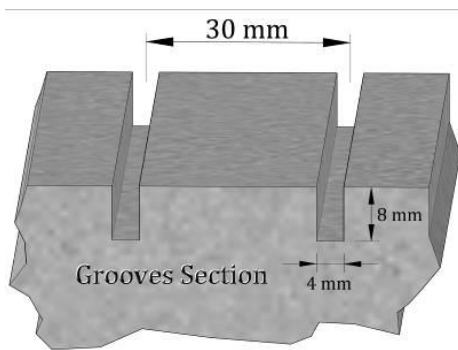

Details \ Zone	L$_{B1}$	L$_{B2}$	L$_{B3}$	L$_{C1}$	L$_{C2}$	L$_{C3}$	L$_P$
Length (mm)	400	700	300	275	300	275	200
Stirrups Spacing Ø8@ (mm) — SR	50	100	50	50	150	50	50
Stirrups Spacing Ø8@ (mm) — WR RW1 RW2	100	100	50	150	150	50	None

Fig. 1 Details of joints (Dimensions, Properties of longitudinal and tie reinforcements, Stirrups spacing)

A.R. Sattarifard, M.K. Sharbatdar, A. Dalvand   433

Fig. 2 Grooving pattern in specimen RW2

(a) Schematic section

(b) Real section
Fig. 3 Section of grooves in specimen RW2

2.3. FRP strengthening of weak specimens

Weak specimens RW1 and RW2 were retrofitted with two FRP strengthening patterns, regarding requirements of ACI-440 [35-36]. Strengthening pattern of beam, column and panel zone in specimen RW1, is shown in Fig. 4, using only one layer of FRP sheet. As shown in Fig. 4, two U-shaped sheets have been used on both upside and downside of the beam for shear strengthening and confining the compression zones of the beam in cyclic loading, with fibers direction perpendicular to the beam axis. For shear strengthening and confining the panel zone, one U-shaped sheet has been used on the column, so that this sheet is not anchored by the U-shaped sheets of the beam. Also the fibers direction is parallel to the beam axis. Due to easy access to the column in practice, in both upside and downside of the panel zone, a layer of FRP sheet was wrapped with 100 mm overlapping ends around

the column. For strengthening of specimen RW2 with grooved surface, in addition to use strengthening pattern of RW1, flexural strengthening sheets were used on the beam. Strengthening pattern of specimen RW2 is shown in Fig. 5, using two L-shaped sheets on both upside and downside of the beam, in the corner of connection, with fibers parallel to the beam axis.
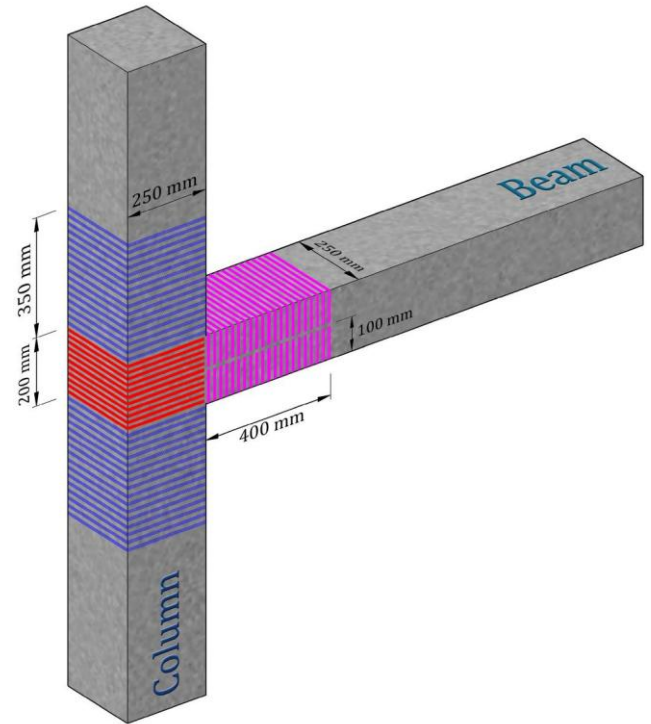

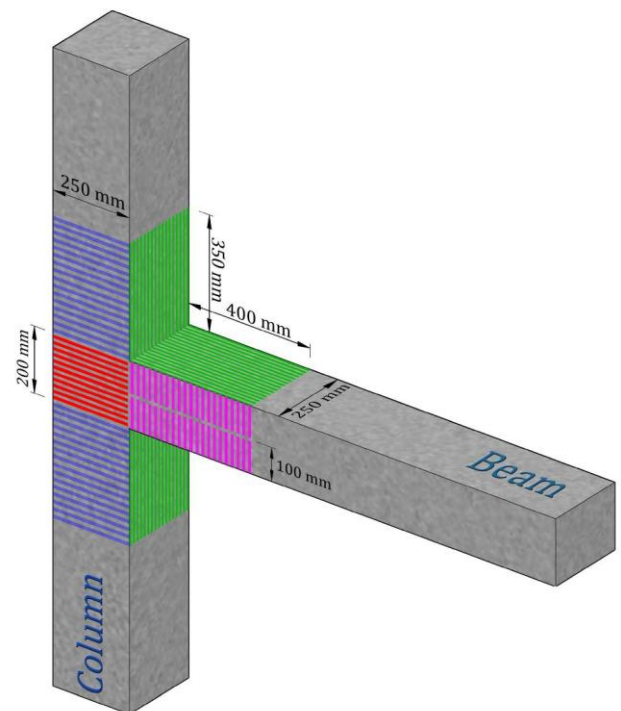**Fig. 4** Shear strengthening of beam and panel zone in specimen RW1

Fig. 5 Shear strengthening of beam and panel zone and flexural strengthening of beam in specimen RW2

One side of L-shaped sheets was installed on upside or downside face (on U-shaped sheet) of the beam and the other side was installed on face (on wrapped sheet) of the column. According to similar researches, applying flexural strengthening on the connection causes early debonding because of high tensile forces and stresses [16-17, 29-33]. So despite this factor in specimen RW2 than RW1, the positive efficiency of grooving method on postponing of debonding is more clearly investigated [34]. It is noteworthy that in all cases, only one layer of FRP sheet was used for strengthening.

2.4. Set-up characteristics

Details of set-up system used for tests are shown in Fig. 6. To determine diagonal strain of panel zone, rotation of beam and to measure displacement at the tip of the beam, some LVDTs[5] were installed on the specimen as shown in Fig. 6. Two 200-kN jacks were used horizontally for cyclic loading on the tip of the beam. For axial loading of the column, a 500-kN jack was installed at the end of the column, in place of roller support, and the other end of the column was restrained to a hinged support. There was 1250 mm distance, from loading point to the column line. During the test, a constant axial load of 410-kN was applied to the column. This axial load is 20% of nominal axial load bearing capacity of the column, calculated from equation 1: $P_0 = 0.85 f_c'(A_g - A_{st}) + A_{st}f_y$ Where f_c' is compressive strength of concrete (MPa), f_y is tensile strength of steel (MPa), Ag is gross sectional area of the column (mm[2]) and Ast is area of steel reinforcements (mm[2]). Drift parameter has been calculated by dividing horizontal displacement of the beam at loading point by distance of loading point to the column line. Horizontal loading of beam was as drift (displacement) control with three cycles of loading in each drift, started from 0.5% drift (6.25 mm displacement) in order to observe first flexural elastic cracks. Increasing cyclic loading history continued up to 8% drift (100 mm displacement), is shown in Fig 7.
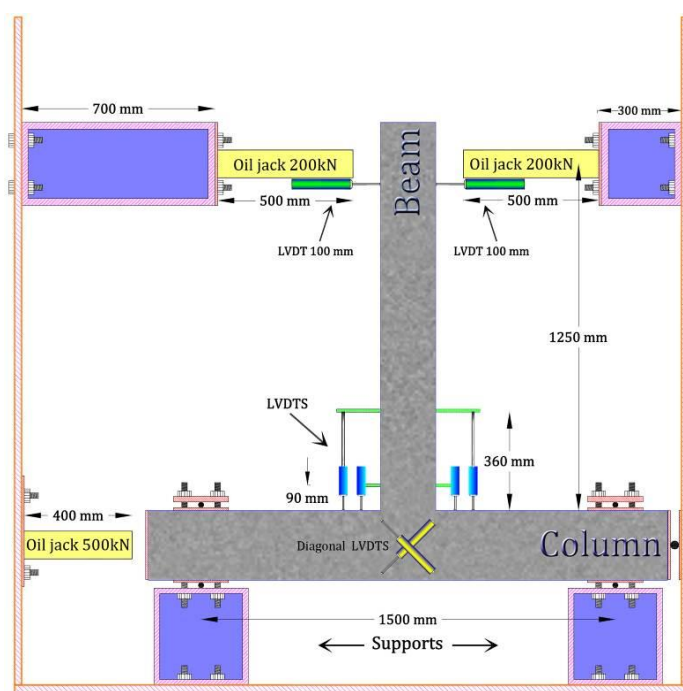
(a) Schematic view
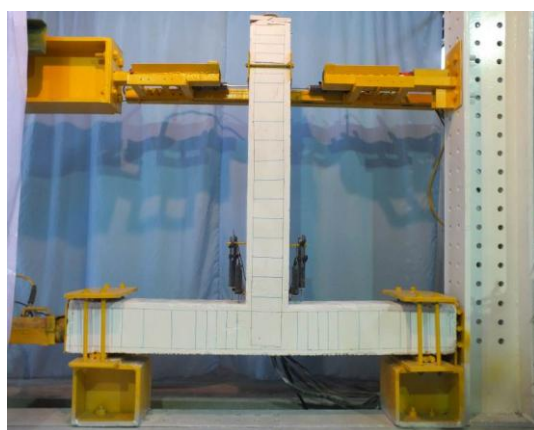
(b) Real view
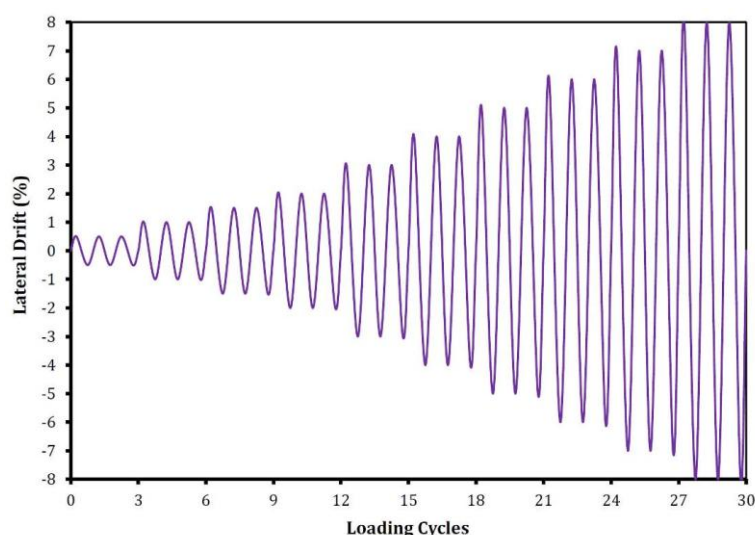**Fig. 6** Scheme of set-up and loading system

Fig. 7 Cyclic lateral loading history with displacement (drift) control

3. Experimental Results

3.1. Observations

As it can be seen from Fig. 8, collapse in specimen WR was in the form of deep flexural cracks at the intersection of beam-to-column. In specimen SR, collapse was in type of formation of flexural plastic hinge and shear cracks with angle 45° in ductile region of the beam. These shear and flexural cracks do not encompass panel zone. Collapse in specimen RW1 was in the form of flexural cracks of beam where it is joined to the column and also collapse in specimen RW2 was in the form of flexural cracks of beam at 50 mm away from where it is joined to the column. Also in this specimen, tearing was seen in flexural strengthening sheets. Deep X-shape shear cracks and crushed concrete of panel zone in specimen WR, are shown in Fig .9.
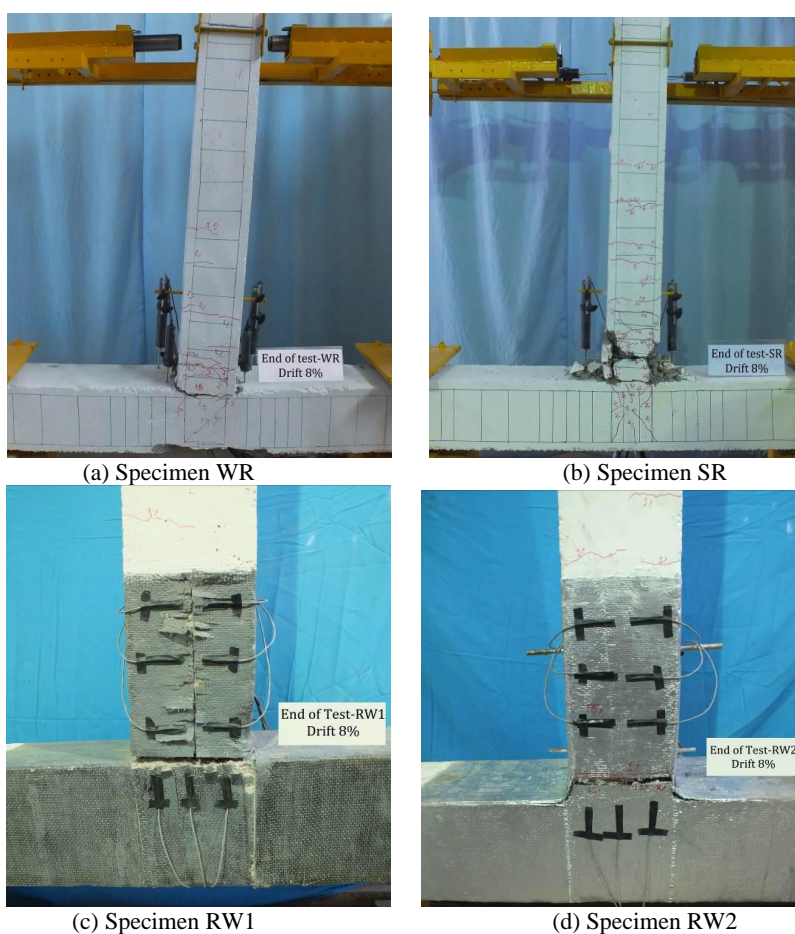

(a) Specimen WR   (b) Specimen SR

(c) Specimen RW1   (d) Specimen RW2

Fig. 8 Collapse form of connections at the end of test

Fig. 9 Crushed concrete of panel zone in specimen WR at the end of test

3.2. Moment-drift behavior

Hysteresis moment-drift curve of specimens are given in Fig. 10, indicating a stable behavior until the end of tests for all specimens. In order to compare the pinching of hysteresis moment-drift curve of specimens, their width in the origin of coordinates are measured as a dimensionless parameter. So specimen SR compared to specimen WR, has

chubbier curve and also the strengthened specimens RW1 and RW2 have chubby hysteresis curves too. Envelope of moment-drift curves for all specimens are shown in Fig. 11, and also review of experimental results are presented in Table 1. Maximum moment (M_{max}) of specimens WR, SR, RW1 and RW2 obtained from Fig. 11, were 23.4, 24.6, 26.4 and 27.1 kN.m, respectively. M_{max} of specimens SR, RW1 and RW2 were 5.4%, 13% and 16% more than that of WR, respectively. Also M_{max} of specimen RW2 was 10% more than that of SR. According to Table 1 and recorded strains, first yielding of longitudinal reinforcements of beams, happened in specimen WR. Yielding moment (M_y) of specimen WR was 13.9 kN.m which was 30% lower than that of SR. Also M_y of specimens RW1 and RW2 were 20.5 and 23.3 kN.m, respectively which were 48% and 68% more than that of WR. According to Table 1, ultimate moment (M_u) corresponding to the maximum displacement before the collapse for specimens WR, SR, RW1 and RW2 were 13.8, 18.3, 22.3 and 26.1 kN.m, respectively. Specimen WR has 40% reduction in M_u than M_{max} compared to 4% reduction in specimen RW2. M_u of specimens SR, RW1 and RW2 increased up to 33%, 61% and 89% compared to WR, respectively.
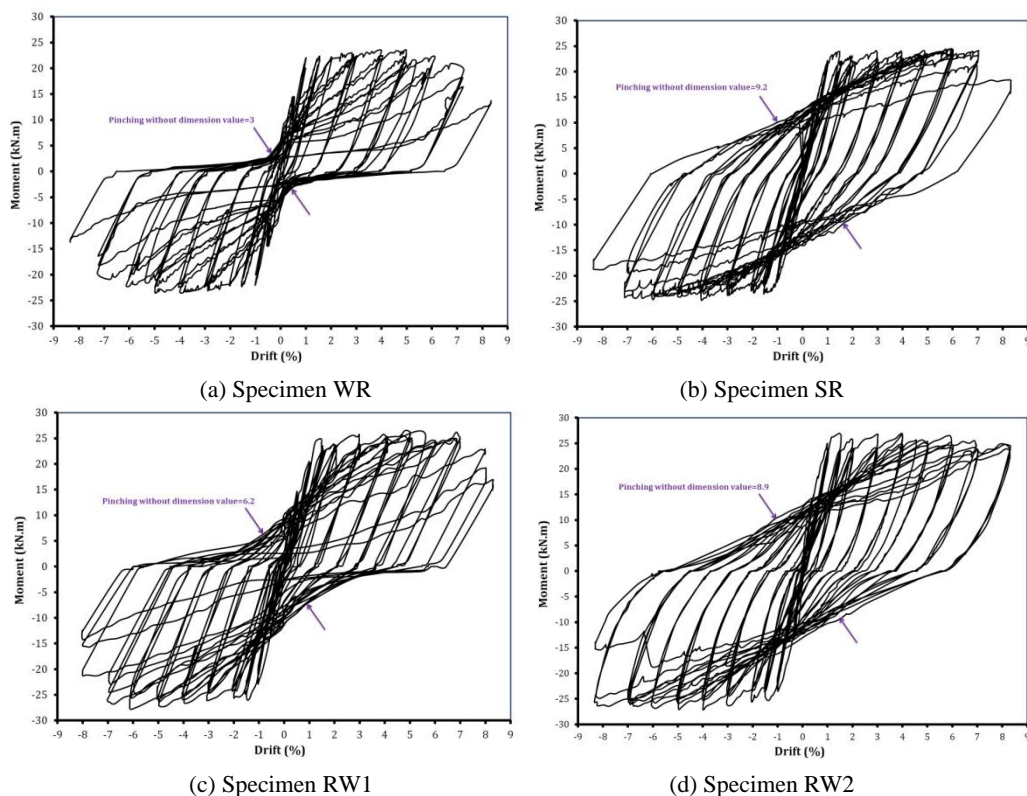

(a) Specimen WR

(b) Specimen SR

(c) Specimen RW1

(d) Specimen RW2

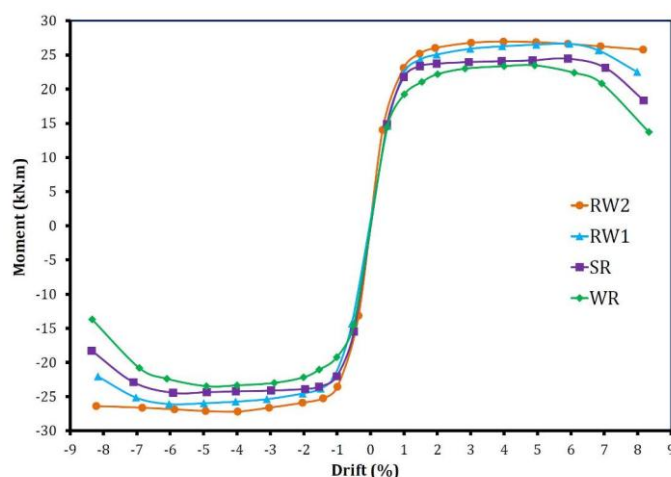**Fig. 10** Hysteresis moment-drift curve of specimens

Fig. 11 Envelope of moment-drift curves

Table 1 Moment Values from Moment-Drift Curves

| Specimen	M_y (kN.m)	M_{max} (kN.m)	M_u (kN.m)	$\dfrac{M_u}{M_{max}}$	Difference compared to WR (%)		Difference compared to SR (%)	
					M_{max}	M_u	M_{max}	M_u
WR	13.85	23.35	13.81	0.6	---	---	-5.2	-24.6
SR	19.72	24.62	18.33	0.74	5.4	32.7	---	---
RW1	20.49	26.38	22.26	0.84	13	61.2	7.1	21.5
RW2	23.29	27.1	26.08	0.96	16.1	88.8	10.1	42.3

3.3. Diagonal strain of panel zone

Moment-diagonal strain curve of specimens WR and SR are shown in Fig. 12. Changes in diagonal strain were measured by cross LVDTs installed in panel zone. Diagonal strain is calculated from dividing changes in length of LVDT by length of it, in any time. Maximum diagonal strain of panel zone in specimens are shown in Table 2. Maximum diagonal strain in specimens WR, SR, RW1 and RW2, were 1.732, 1.012, 0.447 and 0.421%, respectively. Maximum diagonal strain in specimen WR, was 71% more than that of SR. Maximum diagonal strain
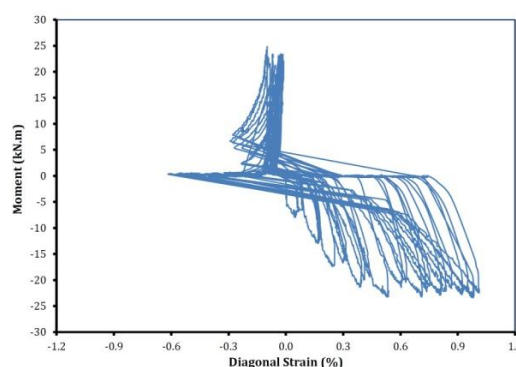
in specimens RW1 and RW2, were 74% and 76% lower than that of WR. Considering the flexural strengthening of specimen RW2, maximum diagonal strain was 6% and 58% lower than specimens RW1 and SR, respectively.

Table 2 Maximum Diagonal Strain of Panel Zone in Specimens

Specimen	Maximum diagonal strain (%)
WR	1.732
SR	1.012
RW1	0.447
RW2	0.421
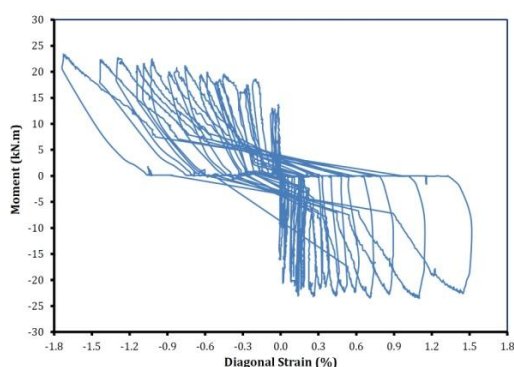
(a) Specimen WR   (b) Specimen SR

Fig. 12 Moment-diagonal strain curve of specimens

4. Discussion

4.1. Ductility, energy absorption and stiffness

Ductility factor of specimens is defined as the ratio of

the ultimate displacement to displacement of first yielding in longitudinal reinforcements of beam ($\Delta u/\Delta y$). To calculate the ductility factor of specimens, the ultimate displacement (Δu) was considered as the minimum of two values: maximum displacement of specimen before

collapse and displacement corresponding to 15% reduction of maximum load. As it is seen in Table 3, displacements in which longitudinal reinforcements were yielded, were defined as (Δy) and for specimens WR, SR, RW1 and RW2 were 10.95, 10.9, 11.3 and 11.2 mm, respectively. The ultimate displacements for specimens WR, SR, RW1 and RW2 were 77.5, 92.3, 97.6 and 99.1 mm, respectively, thereupon ductility factors were equal to 7.07, 8.49, 8.68, and 8.85, respectively. Absorbed energy levels of specimens in every drift of loading are shown in Fig. 13.

Table 3 Ductility factor of Specimens

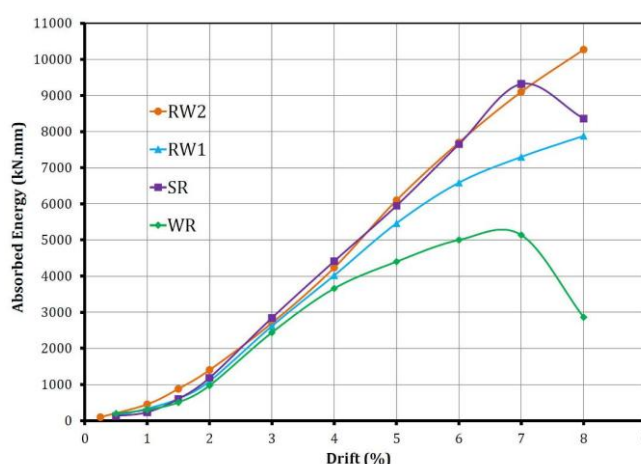| Specimen	Δ_y (mm)	Δ_u (mm)	μ
WR	10.95	77.45	7.07
SR	10.9	92.27	8.49
RW1	11.27	97.55	8.68
RW2	11.2	99.1	8.85

Fig. 13 Energy absorption curve of specimens in loading cycles of every drift

Absorbed energy of connection in every drift of loading can be calculated from the summation of area of hysteresis loops, in which peak load is not lower than 85% of maximum load bearing capacity of connection. All specimens had low and close energy absorption up to 2% drift in comparison to last stages of loading, so that its values for specimens WR, SR, RW1, and RW2 were 970, 1183, 1090, and 1400 kN.mm, respectively. Energy absorption of specimens increased considerably in upper drifts, while energy absorption was nearly the same for all specimens up to 3% drift. Among all specimens, the best strengthened specimen (RW2) and weak designed specimen (WR) had the maximum and the minimum energy absorptions, respectively. Cumulative energy absorptions of specimens up to every drift of loading from the start of test are shown in Fig 14. According to this figure, total absorbed energy of specimen RW2 at the end of the loading was 6%, 69% and 19% more than specimens SR, WR and RW1, respectively. Stiffness values of specimens in every drift are shown in Fig 15. Stiffness value of connection in every drift is equal to the slope of passing line through positive and negative peaks of loading cycles in every drift. According to the figure, up to 1.5% drift, specimen RW2 had more stiffness than others. From a drift of 1.5% to 8%, Stiffness curve of specimens were nearly the same. Stiffness degradation of specimens compared to initial stiffness (in 0.5% drift), are shown in Fig. 16. According to these curves, specimen RW2 showed more stiffness degradation, because of its higher initial stiffness, as seen in Fig 15, stiffness degradation rate of all specimens are nearly the same.
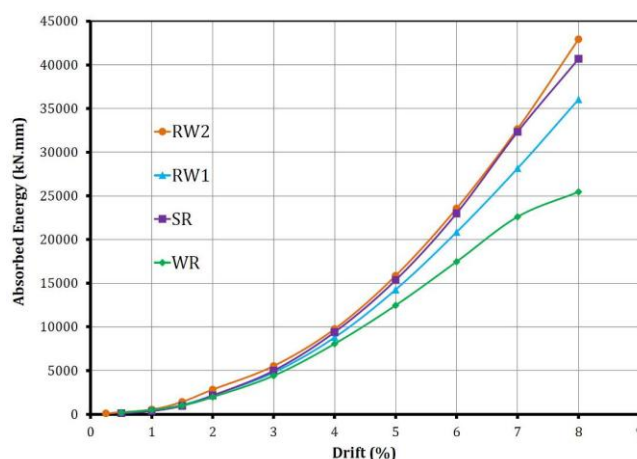

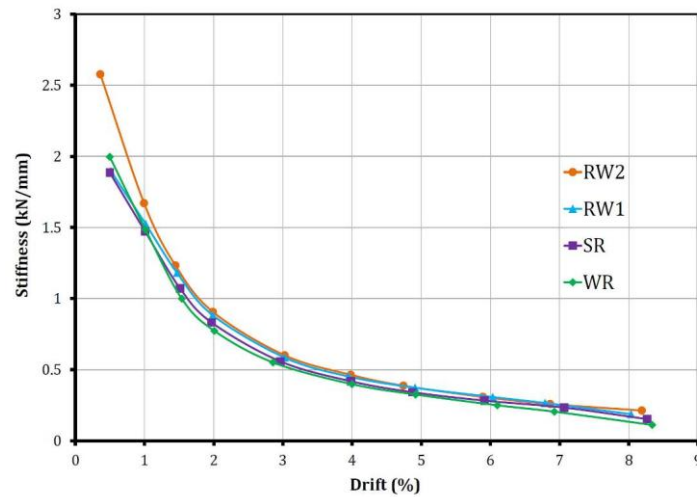**Fig. 14** Cumulative energy absorption curve of specimens

A.R. Sattarifard, M.K. Sharbatdar, A. Dalvand

439

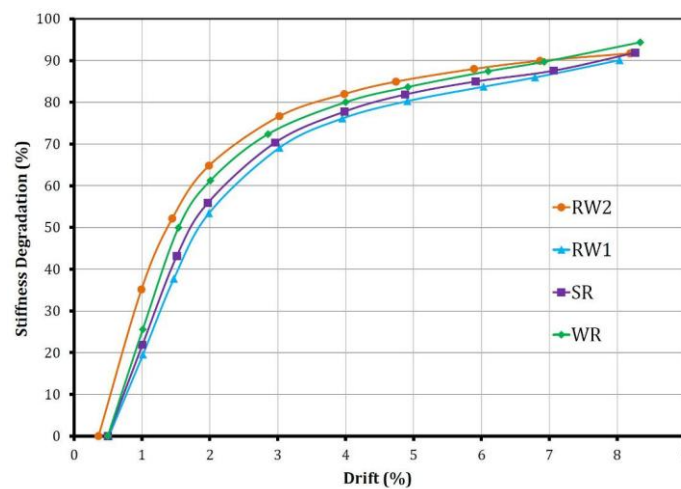**Fig. 15** Stiffness curve of specimens in every drift

Fig. 16 Stiffness degradation curve of specimens in every drift

4.2. Influences of ties spacing

Damage levels are shown in Fig.17 for specimens WR and SR. According to this figure, for specimen SR, in which moderate ductility requirements (for ties spacing) had been regarded correctly, only slight shear cracks were seen in the panel zone. In critical region of the beam, shear and flexural cracks appeared at 200 mm from the panel zone. In the specimen WR, severe shear cracks occurred in the panel zone so that the concrete surface and core of the connection collapsed (Fig. 9 and Fig. 17a). Meanwhile at the intersection of beam-to-column, severe flexural cracks formed and extended in the entire beam section. Yielding, maximum and ultimate strength of specimen WR compared to specimen SR decreased 30%, 5% and 25%, respectively. As it could be seen in Fig. 10, hysteresis moment-drift curve of specimen SR is chubby and fusiform and its width is 9.2 units in the origin of coordinates. While the curve of specimen WR has a significant pinching and its width in the origin of coordinates is 3 units. Without considering the requirements of ties spacing, ductility of specimen WR decreased about 17%, compared to specimen SR. Because of equal flexural capacity of beams in specimens WR and

SR, their stiffness curves were approximately the same. Total absorbed energy of specimen SR at the end of loading was 1.6 times the WR's.

4.3. Effects of retrofitting weak specimens with FRP sheets

Damage levels of specimens RW1 and RW2 are shown in Fig. 18. Due to using strengthening sheets in the panel zone, no shear cracks were observed in specimens, and also no collapse in the form of flexural cracks at the intersection of beam-to-column. The pinching in hysteresis moment-drift curve of specimen RW1 is lower than that of WR, while the curve of specimen RW2 has no pinching and is chubby and fusiform. Also, width of curve for specimen WR is 3 units in the origin of coordinates, while this parameter for specimens RW1 and RW2 are 6.2 and 8.9 units, respectively. In comparison with specimen WR, yielding, maximum and ultimate strength increased respectively 48%, 13% and 61% in specimen RW1, and 68%, 16% and 89% in specimen RW2. Because of flexural strengthening in specimen RW2, yielding and ultimate strength increased by 14%, 17% respectively, compared to specimen RW1. Comparing the ratio of ultimate load to maximum load of specimens showed that the strength

reduction of specimen RW2 was lower than others, especially in high displacements. Ductility of specimens RW1 and RW2 were 22% and 25% more than WR's, also

total absorbed energy of specimens RW1 and RW2 were 1.42 and 1.69 times the WR's.
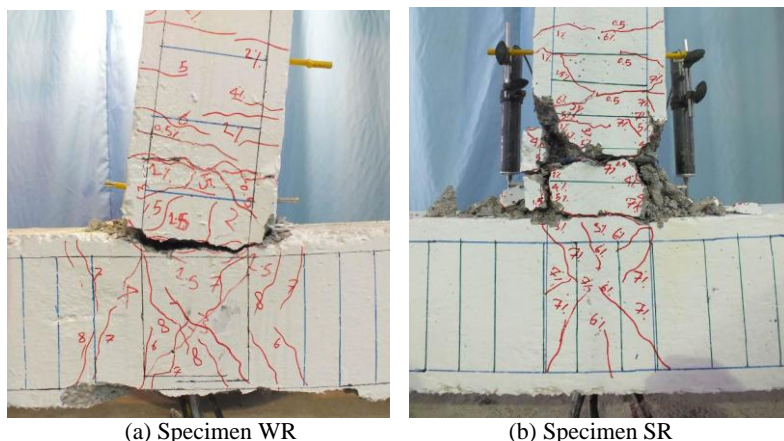

| (a) Specimen WR | (b) Specimen SR |

Fig. 17 Damages level in reference specimens WR and SR at the end of tests
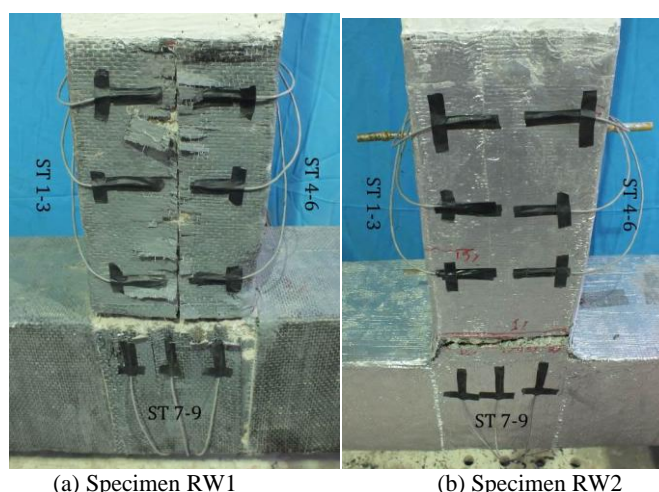

| (a) Specimen RW1 | (b) Specimen RW2 |

Fig. 18 Damages and debonding level in strengthened specimens RW1 and RW2 at the end of tests

4.4. Effects of retrofitting compared to standard reference specimen

According to the previous section, strengthening pattern of specimen RW2 is more effective than RW1's for improving strength properties of retrofitted weak connections. As seen in Fig. 10, width of moment-drift curve of specimens SR and RW2 are 9.2 and 8.9 units, respectively. So both specimens have high ductility, energy absorption and dissipation ability. According to Table 1, yielding, maximum and ultimate strength of specimen RW2 are respectively 18%, 10% and 42% more than those of specimen SR. The ratio of ultimate load to maximum load is 0.74 in SR and 0.96 in RW2, So strength reduction of RW2 is lower than SR's, especially in high displacements. Also, initial stiffness and ductility of RW2 are 37% and 4% more than those of SR, respectively. Energy absorption capacities of these two specimens are nearly the same, up to 7% drift. This means that strengthening pattern of specimen RW2 improves the behavior and strength properties of weak connections, even above the standard reference connection (SR).

4.5. Effects of grooving method on postponing the early debonding

To study the effects of grooving pattern on preventing the debonding of FRP sheets, some strain gauges were installed at the two ends of U-shaped sheets in the beam and panel zone. These strain gauges and also debonding levels of the strengthening sheets in specimens RW1 and RW2, are shown in Fig.18. Maximum strain of FRP sheets are presented in Table 4, so that in specimen RW1, maximum strain at ends of the sheets was 0.49%, which was much less than ultimate tensile strain of FRP sheets (1%). Also, some regions near the end of the sheets were debonded and by increasing strains, progressive debonding was observed in these regions. The maximum strain recorded in RW1 was close to recommended level by design codes for allowed strain of FRP sheets (equal to 0.4%) [34]. So, by increasing the load and according to strains lower than ultimate tensile strain, there was the probability of complete debonding of sheets before rupturing. In specimen RW2, strain at the end of sheets reached to 0.97%, close to ultimate tensile strain of sheets

but almost twice of allowed level by design code (0.4%). Also, no debonding was observed in this specimen. Therefore, by increasing load and reaching higher strains at FRP sheets, there was the probability of complete rupturing at sheets without debonding. So, it is observed that despite applying flexural strengthening in specimen RW2 (which is an effective factor for early debonding and damages in panel zone [16-33]), debonding situation of sheets in RW2 has improved, and this confirms the efficiency of grooving method. By using grooving method, adherence and bonding strength of FRP sheets with concrete surface increases. So, FRP sheets will reach their ultimate tensile strength (strain) and end in rupturing without debonding.

Table 4 Maximum Strain at the ends of U-Shaped Sheets

Specimen	Strengthening sheets in critical region of the beam		Strengthening sheets in panel zone	Ultimate tensile strain	Allowed strain in design code
	ST 1-3	ST 4-6	ST 7-9		
RW1	0.49%	0.47%	0.42%	1%	0.4%
RW2	0.95%	0.97%	0.9%		

5. Conclusions

By comparing experimental results of four RC connections (standard & weak reference specimens and two weak specimens retrofitted with FRP sheets) the following results were concluded:

- Pinching in hysteresis moment-drift curve of specimen RW1 is lower than specimen WR. Whereas no pinching is observed in curve of specimen RW2. The energy absorption of specimens RW1 and RW2 were 42% and 69% more than that of specimen WR, respectively. The ratio of ultimate load to maximum load in specimens RW1 and RW2 were 0.84 and 0.96, respectively.
- In the final stages of loading in specimen RW1, maximum strain of U-shaped sheets reached 0.49% (close to design code value but half the ultimate tensile strain). Also, some regions at the ends of the sheets were debonded and by increasing strains, progressive debonding was observed in these regions. But in specimen RW2, even no slight debonding was observed and maximum strain of sheets was 0.97%, close to ultimate tensile strain and twice the value recommended by design code.
- In comparison with specimen RW1, specimen RW2 had better performance in improving all strength parameters. Grooving method used for installing strengthening sheets in specimen RW2, was completely effective in increasing adherence and bonding strength of FRP sheets with concrete surface, and therefore prevented their early debonding.
- By strengthening specimen RW2, severe damages in ductile regions of the beam and panel zone were prevented, so that similar to specimen SR, its damage level in these regions was slight and did not threaten the safety of the structure. In strengthened specimen RW2, initial stiffness, yielding load of longitudinal reinforcements of the beam, maximum load, ultimate load and ductility increased by 37%, 18%, 10%, 42% and 4%, respectively compared to standard specimen SR. The ratio of ultimate load to maximum load was 0.96 in specimen RW2, but it was 0.74 in specimen SR that shows more strength reduction in last stages of loading. Also their energy absorptions were nearly the same. Retrofitting pattern of specimen RW2, simulated cyclic behavior of specimen SR in strengthened weak connection. Therefore, by applying this retrofitting method, strength parameters of weak connection can be upgraded to standard connection (in which the moderate ductility requirements of design code have been considered), without the risk of early debonding of sheets before rupturing by surface grooves.

Notes

1. High Performance Fiber Reinforced Cementitious Composites
2. Near Surface Mounted Reinforcement
3. Cylindrical strength class=30 MPa
4. Mean values from tensile test of bars
5. Linear variable differential transformer

References

[1] ACI Committee 318. Building code requirements for structural concrete (ACI 318-08), MI, 2008.
[2] ACI-ASCE Committee 352. Recommendation for Design of Beam-Column Joints in Monolithic Reinforced Concrete Structures (ACI 352R-02), 2002.
[3] Parvin A, Altay S, Yalcin C, Kaya O. CFRP rehabilitation of concrete frame joints with inadequate shear and anchorage details. ASCE Journal of Composites for Construction, 2010, No. 1, Vol. 14, pp. 72-82.
[4] Prota A, Nanni A, Manfredi G, Cosenza E. Selective upgrade of underdesigned reinforced concrete beam-columns joints using carbon FRP, Structural Journal, 2004, No. 5, Vol. 101, pp. 699-707.
[5] Sasmal S, Ramanjaneyulua K, Novákb B, Srinivasa V, Kumara K, Korkowskib C, Roehmb C, et al. Seismic retrofitting of non-ductile beam-column sub-assemblage using FRP wrapping and steel plate jacketing, Construction and Building Materials, 2011, No. 1, Vol. 25, pp. 175-82.

[6] Tsonos AG. Effectiveness of CFRP-jackets and RC-jackets in post-earthquake and pre- earthquake retrofitting of beam–column subassemblages, Engineering Structures, 2008, No. 3, Vol. 30, pp. 777-93.

[7] Tsonos AG. Seismic rehabilitation of reinforced concrete joints by the removal and replacement technique, European Earthquake Engineering, 2001, Vol. 3, pp. 29-43.

[8] Karihaloo BL, Benson SDP, Didiuk PM, Fraser SA, Hamill N, Jenkins TA. Retrofitting damaged RC beams with HPFRCC, In Proceedings of the Concrete Communication Conf. Birmingham, UK, British Cement Association, 2000, pp. 153-164.

[9] Karihaloo BL, Alaee FJ, Benson SDP. A new technique for retrofitting damaged concrete structures, Proceedings of the Institution of Civil Engineers: Structures and Buildings, 2002, No. 4, Vol. 152, pp. 309-318.

[10] Maheri MR, Karihaloo B, Alaee FJ. Seismic performance parameters of rc beams retrofitted by cardifrc, Engineering Structures, 2004, Vol. 26, pp. 2069-2079.

[11] Karayannis CG, Chalioris CE, Sideris KK. Effectiveness of beam-column connection repair using epoxy resin injections, Earthquake Engineering, 1998, No. 2, Vol. 2, pp. 217-240.

[12] Hussain M, Sharif A, Basenbul IA, Baluch MH, Al-Sulaimani GJ. Flexural behaviour of precracked reinforced concrete beams strengthened externally by steel plates, Structural Journal, 1995, No. 1, Vol. 92, pp. 14-22.

[13] Sharbatdar MK, Kheyroddin A, Emami E. Cyclic performance of retrofitted RC beam–column joints using steel prop, Construction and Building Materials, 2012, Vol. 36, pp. 287-94.

[14] Ahmed A A, Naganathan S, Nasharuddin K, Fayyadh MM. Repair effectiveness of CFRP and steel plates in RC beams with web opening: effect of plate thickness, International Journal of Civil Engineering, 2015, No. 2, Vol. 13, Transaction A: Civil Engineering.

[15] Eshghi S, Zanjanizadeh V. Repair of earthquake-damaged square r/c columns with glass fiber- reinforced polymer, International Journal of Civil engineering, 2007, No. 3, Vol. 5, pp. 210-223.

[16] El-Amoury T, Ghobarah A. Seismic rehabilitation of beam–column joint using GFRP sheets, Engineering Structures, 2002, No. 11, Vol. 24, pp. 1397-407.

[17] Alsayed SH, Al-Salloum YA, Almusallam TH, Siddiqui NA. Seismic response of frp-upgraded exterior RC beam-column joints, ASCE Journal of Composites for Construction, 2010, No. 2, Vol. 14, pp. 195-208.

[18] Parvin A, Granata P. An experimental study on Kevlar strengthening of beam-column connections, Composites, 2001, Part B, No. 2, Vol. 53, pp. 163-71.

[19] Antonopoulos CP, Triantafillou TC. Experimental investigation of frp-strengthened rc beam-column joints, ASCE Journal of Composites for Construction, 2003, No. 1, Vol. 7, pp. 39-49.

[20] Ghobarah A, Said A. Shear strengthening of beam-column joints, Engineering Structures, 2002, Vol. 24, pp. 881-888.

[21] Mahini SS, Ronagh HR. Strength and ductility of FRP web-bonded RC beams for the assessment of retrofitted beam-column joints, Composite Structures, 2010, Vol. 92, pp. 1325-32.

[22] Al-Salloum YA, Almusallam TH, Alsayed SH. Seismic behavior of AS-built, ACI-complying, and CFRP repaired exterior RC beam-column joints, ASCE Journal of Composites for Construction, 2011, No. 4, Vol. 15, pp. 522-34.

[23] Sharbatdar MK. Monotonic and cyclic loading of new FRP reinforced concrete cantilever beams, International Journal of Civil Engineerng, 2008, No. 1, Vol. 6, pp. 58-71.

[24] Hojatkashani A, Kabir MZ. Experimental examination of CFRP strengthened RC beams under high cycle fatigue loading, International Journal of Civil Engineering, 2012, No. 4, Vol. 10.

[25] Khalou AR, Gharachorlou A. Numerical analysis of RC beams flexurally strengthened by CFRP laminates, International Journal of Civil Engineering, 2005, No. 1, Vol. 3. pp. 1-9.

[26] Jalali M, Sharbatdar MK, Chen J, Jandaghi Alaee F. Shear strengthening of RC beams using innovative manually made NSM FRP bars, Construction and Building Materials, 2012, Vol. 36, pp. 990-1000.

[27] AL-Mahmoud F, Castel A, François R, Tourneur C. Strengthening of RC members with near-surface mounted CFRP rods, Composite Structures, 2009, No. 2, Vol. 91, pp. 138-147.

[28] Esfahani MR. Effect of cyclic loading on punching shear strength of slabs strengthened with carbon fiber polymer sheets, International Journal of Civil Engineering, 2008, No. 1, Vol. 6. pp. 208-215.

[29] Kamada T, Li VC. The effects of surface preparation on the fracture behaviour of ECC/concrete repair system, Cement & Concrete Composites, 2000, No. 6, Vol. 22, pp. 423-431.

[30] Toutanji T, Ortiz G. The effect of surface preparation on the bond interface between FRP sheets and concrete members, Composite Structures, 2001, No. 4, Vol. 53, pp. 457-462.

[31] Oh H, Sim J. Interface debonding failure in beams strengthened with externally bonded GFRP, Composite Interfaces Journal, 2004, No. 1, Vol. 11, pp. 25-42.

[32] Pimanmas A, Pornpongsaroj P. Peeling behaviour of reinforced concrete beams strengthened with CFRP plates under various end restraint conditions, Magazine of Concrete Research, 2004, No. 2, Vol. 56, pp. 73-81.

[33] Malek AM, Saadatmanesh H, Ehsani MR. Prediction of failure load of R/C beams strengthened with FRP plate due to stress concentration at the plate end, Structural Journal, 1998, No. 1, Vol. 95, pp. 142-152.

[34] Mostofinejad D, Mahmoudabadi E. Grooving as an alternative method of surface preparation to postpone debonding of FRP laminates in Concrete Beams, Composites for Construction, ASCE, 2010, http://dx.doi.org/10.1061/(ASCE)CC. 1943-5614.0000117.

[35] American Concrete Institute. ACI Committee 440. Guide for the design and construction of externally bonded FRP system for strengthening concrete structures, MI, Farmington Hills, ACI 440.2R-08, 2008.

[36] Akguzel U, Pampanin S. Assessment and design procedure for the seismic retrofit of reinforced concrete beam-column joints using FRP composite materials, ASCE Journal of Composites for Construction.